



Key Points:

- N_2 fixation rates in Mid-Atlantic Bight shelf waters exceeded those offshore, due in part to elevated diazotroph biomass
- The contribution of diazotrophy to community nitrogen turnover was elevated in frontal waters relative to shelf and offshore waters
- A shelf-water streamer induced by an impinging warm-core ring drove a large flux of newly fixed nitrogen into the Slope Sea

Supporting Information:

Supporting Information may be found in the online version of this article.

Correspondence to:

C. R. Selden, M. R. Mulholland and P. D. Chappell,
 crselden@marine.rutgers.edu;
 mmulholl@odu.edu;
 dreux@usf.edu

Citation:

Selden, C. R., Mulholland, M. R., Crider, K. E., Clayton, S., Macías-Tapia, A., Bernhardt, P., et al. (2024). Nitrogen fixation at the Mid-Atlantic Bight shelfbreak and transport of newly-fixed nitrogen to the Slope Sea. *Journal of Geophysical Research: Oceans*, 129, e2023JC020651. <https://doi.org/10.1029/2023JC020651>

Received 30 OCT 2023

Accepted 12 MAR 2024

Author Contributions:

Conceptualization: C. R. Selden, M. R. Mulholland, S. Clayton, D. J. McGillicuddy Jr., W. G. Zhang, P. D. Chappell
Data curation: C. R. Selden, K. E. Crider
Formal analysis: C. R. Selden
Funding acquisition: M. R. Mulholland, S. Clayton, D. J. McGillicuddy Jr., W. G. Zhang, P. D. Chappell
Investigation: C. R. Selden, K. E. Crider, A. Macías-Tapia, P. Bernhardt, P. D. Chappell

© 2024. The Authors.

This is an open access article under the terms of the [Creative Commons Attribution License](#), which permits use, distribution and reproduction in any medium, provided the original work is properly cited.

Nitrogen Fixation at the Mid-Atlantic Bight Shelfbreak and Transport of Newly Fixed Nitrogen to the Slope Sea

C. R. Selden^{1,2} , M. R. Mulholland² , K. E. Crider², S. Clayton^{2,3} , A. Macías-Tapia^{2,4}, P. Bernhardt² , D. J. McGillicuddy Jr.⁵ , W. G. Zhang⁵, and P. D. Chappell^{2,6}

¹Department of Marine and Coastal Sciences, Rutgers University, New Brunswick, NJ, USA, ²Department of Ocean and Earth Sciences, Old Dominion University, Norfolk, VA, USA, ³Ocean BioGeosciences, National Oceanography Centre, Southampton, UK, ⁴Now at Office of Education, National Oceanic and Atmospheric Administration, Silver Spring, MD, USA, ⁵Department of Applied Ocean Physics and Engineering, Woods Hole Oceanographic Institution, Woods Hole, MA, USA, ⁶Now at College of Marine Science, University of South Florida, St. Petersburg, FL, USA

Abstract Continental shelves contribute a large fraction of the ocean's new nitrogen (N) via N_2 fixation; yet, we know little about how physical processes at the ocean's margins shape diazotroph biogeography and activity. Here, we test the hypothesis that frontal mixing favors N_2 fixation at the Mid-Atlantic Bight shelfbreak. Using the $^{15}\text{N}_2$ bubble release method, we measured N_2 fixation rates on repeat cross-frontal transects in July 2019. N_2 fixation rates in shelf waters (median = $5.42 \text{ nmol N L}^{-1} \text{ d}^{-1}$) were higher than offshore ($2.48 \text{ nmol N L}^{-1} \text{ d}^{-1}$) but did not significantly differ from frontal waters ($8.42 \text{ nmol N L}^{-1} \text{ d}^{-1}$). However, specific N_2 uptake rates, indicative of the relative contribution of diazotroph-derived N to particulate N turnover, were significantly higher in frontal waters, suggesting that diazotroph-derived N is of greater importance in supporting productivity there. This study furthered captured an ephemeral shelf-water streamer, which resulted from the impingement of a warm core ring on the shelf. The streamer transported shelf-water diazotrophs (including UCYN-A and *Richelia* spp., as assessed by qPCR) offshore with sustained high N_2 fixation rates. This feature injected >50 metric tons d^{-1} of newly fixed N to the Slope Sea—a rate equivalent to $\sim 4\%$ of the total N flux estimated for the entire Mid-Atlantic Bight. As intrusions of Gulf Stream meanders and eddies onto the shelf are increasing in frequency due to climate change, episodic lateral fluxes of new N into the Slope Sea may become increasingly important to regional budgets and ecosystem productivity.

Plain Language Summary Nitrogen limits photosynthetic growth, and thus CO_2 drawdown, across vast areas of the world's ocean. This limitation can be relieved through N_2 fixation—the conversion of N_2 gas to a bioavailable form of N by a select group of microbes. Historically, marine N_2 fixation has largely been ascribed to microbes living in and adapted to (sub)tropical waters of the central ocean basins where concentrations of bioavailable N are exceedingly low. Yet, recent work has demonstrated that significant N_2 fixation occurs on the continental shelves as well, with implications for both local and global N budgets. Here, we present a case study from the Mid-Atlantic Bight, conducted in July 2019, which shows that N_2 fixation rates were significantly higher in shelf waters than offshore. We found that short-lived physical transport processes can move these active shelf-water communities offshore as they continue to fix N_2 . In the singular export event captured by this study, which lasted only a few days, shelf-water N_2 -fixers added roughly 4% of the total annual bioavailable N flux to the low-nutrient offshore waters. Because these events are projected to increase in intensity with climate change, shelf-water N_2 -fixers may become increasingly important in fueling productivity in the ocean's central basins.

1. Introduction

Marine dinitrogen (N_2) fixation, the microbially mediated conversion of N_2 gas to ammonia, fuels ocean productivity both globally and locally. On a global scale, N_2 fixation is the primary mechanism by which the ocean's fixed nitrogen (N) inventory is replenished, compensating for fixed N losses via denitrification and anammox (Gruber & Galloway, 2008). On local scales, N_2 fixation relieves N limitation across vast swaths of the world's ocean (Moore et al., 2013). By enabling CO_2 drawdown, N_2 fixation is thought to profoundly influence global climate on geologic timescales (Falkowski et al., 1998; Gruber, 2004; Hutchins et al., 2007).

The environmental factors that regulate the distribution and activity of N_2 fixing microbes (diazotrophs) remain poorly constrained, hampering efforts to close the global N budget and effectively model regional

Methodology: C. R. Selden, M. R. Mulholland, P. Bernhardt, P. D. Chappell

Project administration: C. R. Selden, M. R. Mulholland, P. Bernhardt, D. J. McGillicuddy Jr., P. D. Chappell

Resources: M. R. Mulholland, P. D. Chappell

Supervision: C. R. Selden, M. R. Mulholland, D. J. McGillicuddy Jr., W. G. Zhang, P. D. Chappell

Visualization: C. R. Selden

Writing – original draft: C. R. Selden

Writing – review & editing: C. R. Selden, M. R. Mulholland, K. E. Crider, S. Clayton, A. Macías-Tapia, P. Bernhardt, D. J. McGillicuddy Jr., W. G. Zhang, P. D. Chappell

biogeochemistry. Early marine work focused largely on N_2 fixation in severely N-limited ocean basins, identifying the filamentous cyanobacterium *Trichodesmium* as the major contributor to new N inputs (e.g., Capone et al., 1997; Dugdale, 1961; Dugdale et al., 1964). *Trichodesmium* is highly active in N-depleted waters where phosphorus and iron, a key constituent of the nitrogenase enzyme which mediates N_2 fixation, are available. Subsequent development and broad application of both molecular and microscopic approaches led to the identification of numerous other diazotrophs which differ in their biogeography (Zehr & Capone, 2020), including several symbiotic diazotrophic clades residing within diatom (Carpenter et al., 1999; Schvarcz et al., 2022) and haptophyte (Thompson et al., 2012) hosts. These groups are thought to be less sensitive to ambient dissolved inorganic N (Zehr & Capone, 2020) and, in some cases, appear to thrive in coastal upwelling systems (e.g., Mills et al., 2020; Selden et al., 2022; Voss et al., 2006), potentially extending the life of phytoplankton blooms where ambient N is drawn down in advance of other nutrients. Realization that these organisms significantly augment ocean fixed N inputs, and that community N_2 fixation in many systems is less sensitive to ambient N than previously thought (Knapp, 2012; Mulholland & Capone, 2000; Mulholland et al., 2001) has led to increased interest in coastal N_2 fixation.

Though N_2 fixation on continental shelves remains drastically under-sampled globally, recent work from the western North Atlantic Ocean has established that it contributes significantly to the N budget of this basin (Mulholland et al., 2012, 2019; Selden, Chappell, et al., 2021; Tang et al., 2019, 2020). Mulholland et al. (2019) estimated that a small swath of the continental shelf from the Mid-Atlantic Bight (MAB) to the Gulf of Maine, which accounts for only 6.4% of the total shelf area around the North Atlantic, contributed 0.28 Tg N yr⁻¹. This value represents >7% of total new N inputs to the North Atlantic basin (Capone et al., 2005; Mahaffey et al., 2005) and is equivalent to the fixed N contribution previously estimated for the entire North Atlantic shelf (Nixon et al., 1996). Indeed, N_2 fixation rates on the Mid- and South Atlantic Bight continental shelves (<200 m) are typically an order of magnitude greater than comparable measurements offshore, largely due to higher biomass (Selden, Chappell, et al., 2021). However, both high biomass and high specific N_2 uptake rates—a value representing the relative contribution of N_2 fixation to community turnover of particulate N (PN)—were observed near the Cape Hatteras front, resulting in exceptionally high N_2 fixation rates in August 2016 (Selden, Chappell, et al., 2021). Similarly, high N_2 fixation rates were observed near the shelfbreak front south of New England in June 2011 (Mulholland et al., 2019).

Density fronts in the ocean profoundly influence ocean ecology and biogeochemical cycling due, in part, to their role as so-called “nutrient gateways”, guarding exchange of materials between chemically distinct waters (Palter et al., 2013). In Western Boundary Current regions like the western North Atlantic, the distinct environmental characteristics of frontal waters enhance plankton diversity and favor opportunist taxa, including diatoms, by injecting nutrients into euphotic ocean waters (Clayton et al., 2014; Mangolte et al., 2022; Oliver et al., 2021). Recent observations (e.g., Bourbonnais et al., 2009; Lu et al., 2019; Mulholland et al., 2019; Selden, Chappell, et al., 2021) hint that diazotrophy may be elevated in frontal systems. If so, such an enhancement may be driven by frontal physico-chemical conditions, including along-isopycnal upwelling of nutrients like phosphorus and iron (e.g., due to convergence in the bottom boundary layer; Linder et al., 2004). However, to date, such observations have largely been made at low spatial resolution with relatively few samples collected from true frontal waters. Given the highly dynamic nature of frontal zones, greater spatial and temporal resolution is necessary to assess how diazotroph biogeography and activity may respond to water mass mixing.

This work sought to determine whether shelfbreak frontal dynamics enhance diazotrophy, using the MAB as a case study. The MAB shelfbreak is a productive and bio-physically dynamic region; cool, low-salinity waters of terrestrial and Arctic origin flow southwest alongshore on the shelf, abutting warm, salty Slope Sea waters offshore. The shelf and offshore waters are separated by a semi-persistent shelfbreak front. The front is baroclinically unstable and prone to meanders, which can drive cross-shelf mixing (Zhang & Gawarkiewicz, 2015b). The Gulf Stream, carrying water with temperature and salinity even higher than the Slope Sea, flows north-eastward offshore. Instabilities of the Gulf Stream often develop into large-amplitude meanders or (sub) meso-scale warm core rings, both of which can directly impinge on the MAB shelfbreak, alter the shelfbreak frontal structure, and drive significant water mass exchange between the shelf and the Slope Sea (Gawarkiewicz et al., 2018; Zhang & Gawarkiewicz, 2015a).

In this study, we examined diazotroph activity and biogeography across the shelfbreak front south of New England (the northern end of the MAB) in July 2019. We repeatedly sampled shelf, front, and offshore waters over a

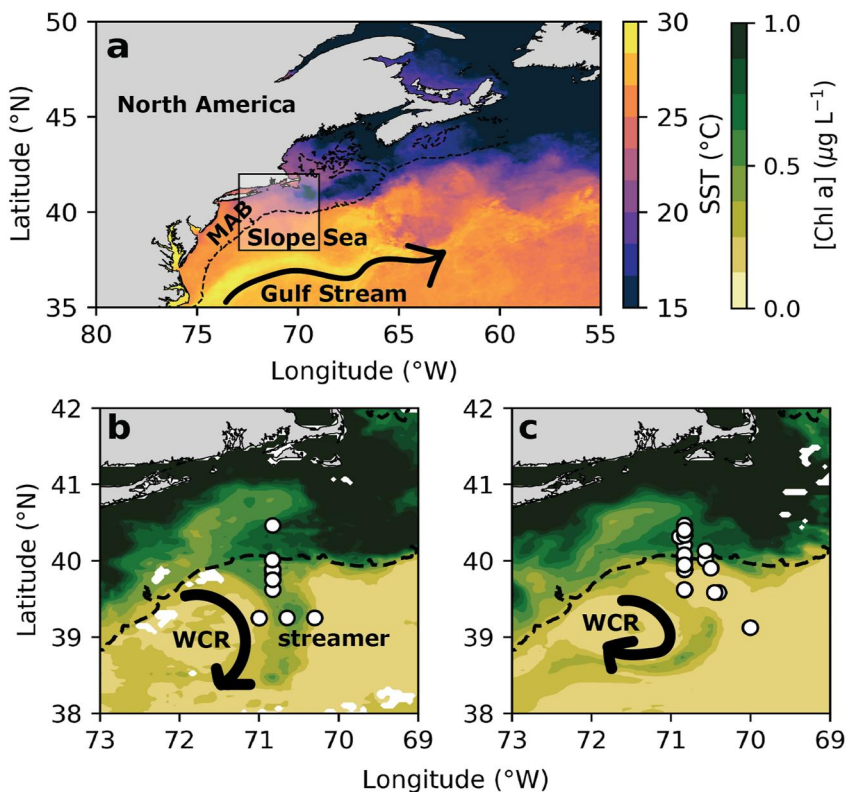


Figure 1. (a) Mean regional sea surface temperature (SST) in July 2019 and 8-day averaged sea surface chlorophyll *a* (Chl *a*) concentrations on (b) 4–11 July and (c) 12–19 July 2019, overlying sampling stations. In panel (a), the box shows the location of panels (b) and (c). The dashed line indicates the 200 m isobath. ‘WCR’ indicates the warm core ring derived from the Gulf Stream. ‘MAB’ indicates the Mid-Atlantic Bight. Data source: MODIS, [NASA Goddard Space Flight Center](#), accessed 27 March 2023.

2-week period. At the beginning of our expedition, we encountered a shelf-water streamer—a thin filament of surface water from the shelf driven offshore into the Slope Sea by the impingement of a warm core ring which spawned off the Gulf Stream (Zhang et al., 2023). We show that N₂ fixation is enhanced in shelf waters, and that these diazotrophic communities remain active as shelf-waters are advected offshore, bringing a significant pulse of newly fixed N into the Slope Sea.

2. Materials and Methods

2.1. Hydrographic Observations

Samples and hydrographic profiles were collected onboard the research vessel (R/V) *Thomas G. Thompson* in July 2019 (Figure 1). We repeatedly occupied a high resolution (7 km) north-south transect at the New England shelfbreak, and collected several additional samples from an east-west transect which crossed over the streamer and other peripheral stations, over a 2 week period (5–17 July; Figure 1). Our transect captured both cool, low salinity MAB shelf waters and warm, salty Slope Sea waters. The first several days of sampling (July 6–8) were devoted to study of the streamer (Figure 1b).

Vertical conductivity-temperature-depth (CTD) profiles were collected using a CTD-rosette equipped with 24 10 L Niskin bottles, a photosynthetically active radiation (PAR) sensor (BioSpherical Instruments), and a chlorophyll *a* fluorometer (WetLabs FLNTURTD). Samples to determine nitrate, phosphate, and silicate concentrations were filtered (0.4 µm, polycarbonate) directly from Niskin bottles in acid-washed polyethylene bottles and stored frozen until analysis via standard colorimetric methods at the WHOI Nutrient Analytical Facility using a SEAL Analytical AA3 HR discrete chemistry analyzer. Detection limits for nitrate, phosphate, and silicate methods were 0.040, 0.030 and 0.009 µM, respectively.

2.2. N₂ Fixation Rate Measurements

N₂ fixation rate measurements were quantified using the bubble release technique (Chang et al., 2019; Klawonn et al., 2015), a variant of the ¹⁵N₂ tracer method (Montoya et al., 1996) which accounts for the slow dissolution time of N₂ gas (White et al., 2020). The particulars of our approach have been recently described (Selden et al., 2019; Selden, Chappell, et al., 2021; Selden, Mulholland, et al., 2021). In brief, whole water from Niskin bottles was collected into 10 L LDPE carboys. To assess the initial isotopic enrichment and mass of PN, three aliquots of this sample (0.1–2 L depending on sample biomass) were filtered through combusted (4 hr, 450°C) glass fiber filters (0.3 µm, GF-75, Advantec) on a ¹⁵N tracer-free filtration rig. These filters were collected in clean microcentrifuge tubes and stored frozen (−20°C) until analysis at Old Dominion University (see below).

To measure ¹⁵N₂ uptake, triplicate PETG bottles (0.5–2 L) were rinsed with whole water then filled, ensuring that no bubbles remained. ¹⁵N₂ gas (~99%, Cambridge Isotope Laboratories) was added using a gas-tight syringe (VICI Precision Sampling) through flexible silicon septa; samples were gently rocked for 15 min as described by Selden et al. (2019). Any remaining bubble was subsequently removed to ensure constant isotopic enrichment over the incubation period, and bottles were incubated on-deck for approximately 24 hr. To avoid temperature-shocking our samples as we moved back-and-forth across the front, which had a very large temperature gradient (~16–26°C), we maintained three on-deck incubators that recirculated water through aquaria chillers (MC-1/10HP, AquaEuroUSA) housed in custom casings (built from King Starboard plastic sheet) for protection and maintained approximate temperature conditions for shelf, frontal, and offshore waters, respectively.

At the end of the incubation period, a 6 ml sample aliquot was collected from each bottle and transferred to a helium-purged Exetainer™ containing 50 µl zinc chloride (50% w/v). These samples were stored at room temperature and upside-down in 15 ml Falcon™ tubes, submerged in ultrapure water, until analysis at the UC Davis Stable Isotope Facility. The remaining incubation volume was then filtered as described above for initial PN samples. Initial and final PN isotopic composition and concentration were analyzed at Old Dominion University on a Europa 20/20 isotope ratio mass spectrometer with an automated N and carbon preparation module. Low mass samples (<10 µg N) were excluded from downstream analysis as IRMS response can become non-linear at low mass (White et al., 2020).

Specific N₂ uptake rates (SUR) were calculated following Montoya et al. (1996):

$$SUR = \frac{(A_{PN_{t=f}} - A_{PN_{t=0}})}{(A_{N_2} - A_{PN_{t=0}})} \times \frac{1}{time} \quad (1)$$

where A represents the atom-% enrichment of the initial ($t = 0$) or final ($t = f$) PN pool, or the N₂ pool. Across all experiments, A_{N_2} averaged $3.89 \pm 2.0\%$; experiments with <1% enrichment were excluded from downstream analysis. The specific uptake rate represents the relative contribution of diazotroph-derived N to PN turnover within a given sample. Absolute N₂ fixation rates (NFR) were calculated as:

$$NFR = SUR \times [PN] \quad (2)$$

where [PN] indicates the PN concentration. Limits of detection and quantification were calculated per incubation by propagating the minimum detectable difference between initial and final ¹⁵N atom-% enrichment of the PN pool (3σ and 10σ , respectively, $n \geq 7$ 12.5 µg N standards measured daily) through Equation 2 (Ripp, 1996; White et al., 2020). A rate was only considered detectable if two of three replicate incubations yielded detectable rates.

2.3. *nifH* Enumeration

To assess diazotroph diversity and abundance, whole water was collected in 4 L acid-washed (10% HCl) polypropylene bottles (Nalgene) and gently filtered via peristalsis onto 0.22 µm cartridge filters (Sterivex™, MilliporeSigma). Filters were preserved by displacing remaining water with air, then filling cartridges with RNAlater™ (Life Technologies) and incubating for 12–18 hr at 4°C before flash-freezing in liquid nitrogen. Samples were stored at −80°C until analysis. DNA was extracted using the AllPrep MiniKit (Qiagen) following manufacturer's protocols but with the addition of a bead-beater step as described in Selden et al. (2022).

The abundances of common diazotrophic clades were quantified in triplicate via quantitative PCR (qPCR) using 2x TaqMan Fast Advanced Master Mix (Applied Biosystems) on a Real-Time PCR system (Applied Biosystems) following Selden et al. (2022). Previously published custom primer/probe sets were employed to quantify the haptophyte-symbionts UCYN-A1 (Church et al., 2005) and UCYN-A2 (Thompson et al., 2014), the diatom-symbionts *Richelia intracellularis*, *Richelia euintracellularis*, and *Richelia rhizosoleniae* (Foster et al., 2007; Selden, Chappell, et al., 2021), and *Trichodesmium* spp. (Selden, Chappell, et al., 2021). Custom synthetic plasmids (GeneWiz) and no-template controls were run in triplicate for each analysis. To calculate effective limits of detection and quantification, we assumed minimum detectable and quantifiable gene concentrations to be 3 and 10 copies reaction⁻¹, respectively (Bustin et al., 2020). Due to variability in sample filtrate volume, which ranged from 1 to 4.3 L depending on sample biomass, detection and quantification limits ranged from 173 to 555 and 578–1,852 gene copies L⁻¹, respectively.

2.4. Statistics

For both rates and gene concentrations, values below the detection and quantification limits were forced equal to zero and the detection limit, respectively, when visualizing data and conducting statistical tests. Groups were compared via one-way analysis of variance (ANOVA). To avoid the assumption of normality, we assessed significance by comparing computed test statistics (*F* values) to those derived from 10,000 random data permutations (Manly, 2006).

3. Results

3.1. Regional Hydrography

To analyze the influence of hydrographic conditions on N₂ fixation activities, we consider three general water masses as characterized by salinity, namely, *shelf waters* with salinity <34 psu, *offshore waters* with salinity >35 psu, and *frontal waters* with salinity 34–35 psu. These categorical designations are consistent with prior work on the New England shelfbreak front (e.g., Gawarkiewicz et al., 1996; Joyce et al., 1992; Zhang et al., 2023). Note that the offshore waters include Slope Sea water and high-salinity ring water originating from the Gulf Stream. The frontal waters here represent intermediate water masses that result from mixing of shelf and offshore waters, and are not solely associated with the shelfbreak front. For instance, due to mixing with the ambient slope and ring waters, much of the water at the edges of the streamer (described below) had salinity between 34 and 35 and was thus categorized in this study as frontal.

In February 2019, five months prior to our study, a warm core ring detached from the Gulf Stream in the continental slope region southeast of Georges Bank (~64°W, 40°N); by March, it was impinging on the MAB shelf (Zhang et al., 2023). As it spun, the ring drew $0.26 \times 10^6 \text{ m}^3 \text{ s}^{-1}$ of high biomass shelf water offshore into the Slope Sea where it manifested as a thin filament ('streamer'; Figure 1b) ~50 km wide and ~200 km long (Zhang et al., 2023). Due to the lower density of shelf water, the streamer stayed in the surface layer overriding offshore water. On the surface, the streamer was bounded to the west by ring water and to the east by Slope Sea water (Figure 1b). Defining *streamer water* as water in the Slope Sea (offshore of the 200 m isobath) with salinity <34.5, the streamer was ~50 m thick at the seaward edge of our sampling area (~80 km offshore of the 200 m isobath) at the beginning of our expedition in July. This feature, which was described in detail by Zhang et al. (2023), displayed heightened primary productivity and caused significant net offshore transport of algal organic carbon (1.2×10^3 metric tons [mton] d⁻¹) to the Slope Sea, and onshore transport of heat and salt. During our expedition, the streamer weakened and shifted to the southwest of our study area (Zhang et al., 2023), leaving shelf waters with high chlorophyll *a* entrained in the Slope Sea (Figure 1c). After persisting for ~5 months, the streamer was finally absorbed into the Gulf Stream at the end of August (Zhang et al., 2023).

In the first days of sampling (July 6–8) our standard north-south transect along 70.8°W (Figure 1), the shelfbreak front—which typically manifests with condensed isopycnals (or isohalines) shoaling offshore and outcropping at the surface (Linder & Gawarkiewicz, 1998)—was absent. Instead, the isopycnals and isohalines were nearly horizontal as a 50 m thick surface layer of shelf water was drawn offshore by the streamer on the eastern periphery of the warm core ring (Zhang et al., 2023). This water mass exhibited low nitrate concentrations, with phosphate concentrations ranging from ~0.1 to 0.4 μM (see Figure 9 in Zhang et al. (2023)). The streamer feature persisted for several days on our north-south transect before migrating westward away along with the warm core ring

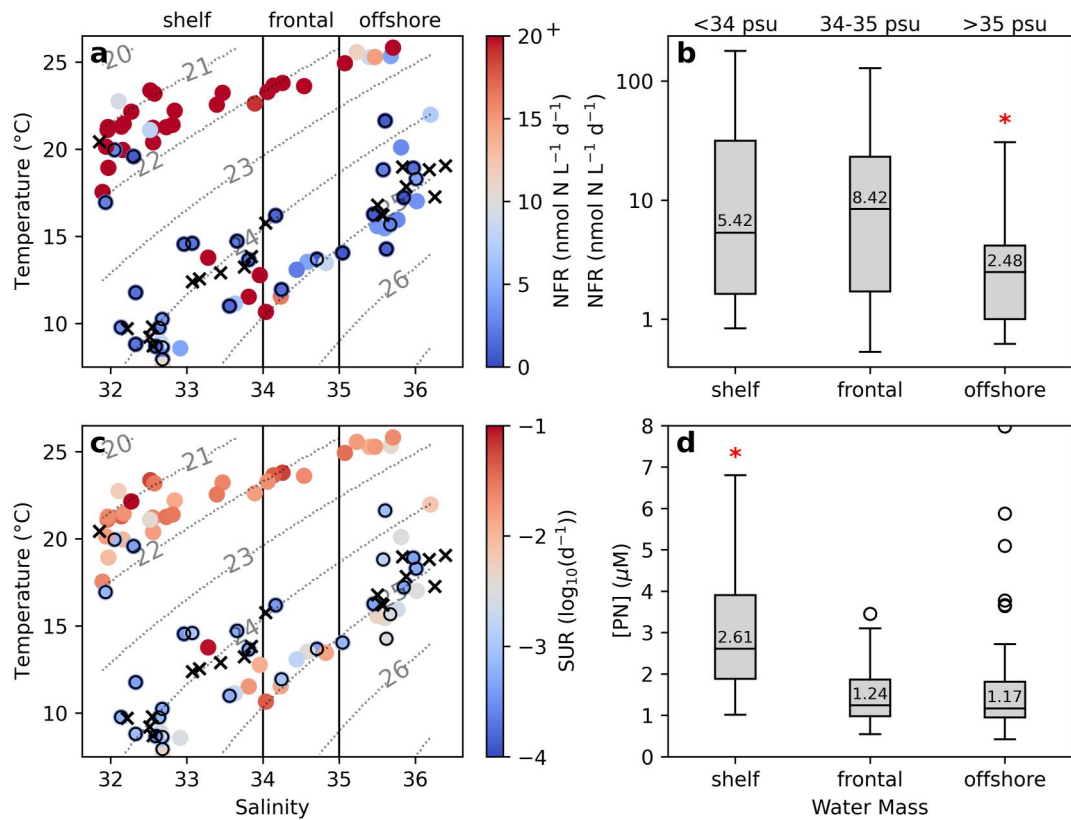


Figure 2. Temperature-salinity diagrams with (a) N_2 fixation and (c) specific N_2 uptake rates depicted as colored dots, and box-and-whisker plots showing range of (b) N_2 fixation rates and (d) particulate nitrogen (PN) concentration within the euphotic zone ($>0.1\%$ surface PAR; $<80\text{ m}$ depth) shelf ($<34\text{ psu}$; $n = 54$), frontal ($34\text{--}35\text{ psu}$; $n = 13$), and offshore ($>35\text{ psu}$; $n = 29$) waters. On panels 'a' and 'c', black circles indicate rates that were detectable but not quantifiable with the color representing the analytical detection limit. Measurements below the limit of analytical detection are denoted by an 'x'. On panels 'b' and 'd', red stars indicate groups that significantly differ (one-way ANOVA; see Table S2 in Supporting Information S1 for pertinent statistics). Printed values give the median for each group; circles show flier values, that is, those greater than 1.5 times the interquartile range.

(Figure 1). Subsequent days of sampling on the north-south transect captured a more typical shelfbreak front with relatively vertical isohalines separating shelf and offshore waters.

In both shelf and offshore waters, the upper mixed layer ($<5\text{ m}$), warmed by high summer solar radiation, exhibited high temperatures (mean $\sim 22.5^\circ\text{C}$). Below this thin surface layer, shelf waters were characterized by low temperatures (mean $\sim 11.6^\circ\text{C}$) relative to offshore waters (mean $\sim 14.8^\circ\text{C}$). Shelf waters also exhibited higher phosphate concentrations (Figure S1 in Supporting Information S1; Figures 9 and 13 in Zhang et al. (2023)), lower nitrate:phosphate ratios (Figure S2 in Supporting Information S1), and higher biomass than offshore waters, as indicated by elevated particulate organic carbon (Figure S3 in Supporting Information S1) and chlorophyll *a* fluorescence (Figure S4 in Supporting Information S1; Figures 8 and 12 in Zhang et al. (2023)).

3.2. N_2 Fixation Rates

Across the study region, N_2 fixation rates ranged from below the limit of analytical detection to $178 \pm 18\text{ nmol N L}^{-1}\text{ d}^{-1}$, with a median rate of $3.30\text{ nmol N L}^{-1}\text{ d}^{-1}$ ($n = 96$ replicated measurements; Table S2 in Supporting Information S1, Figure 2). N_2 fixation was detected in 80.2% of samples ($n = 77$) and was considered quantifiable in 51.0% ($n = 49$). Of the detectable rates, 27.3% ($n = 21$) were measured in waters with nitrate concentrations $>1\text{ }\mu\text{M}$; the median nitrate:phosphate ratio in these samples was ~ 10 .

N_2 fixation rates were exceptionally high ($>100\text{ nmol N L}^{-1}\text{ d}^{-1}$) in four samples from water masses where nitrate was undetectable (i.e., $<0.040\text{ }\mu\text{M}$) but phosphate and silicate remained measurable (>0.009 and $0.030\text{ }\mu\text{M}$,

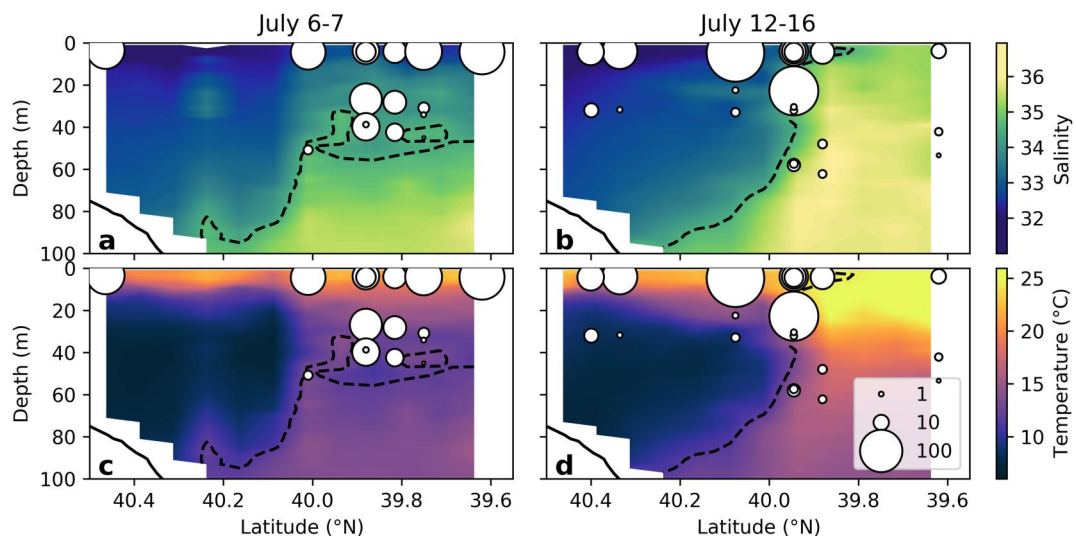


Figure 3. N_2 fixation rates ($\text{nmol N L}^{-1} \text{d}^{-1}$) depicted as sized dots, overlying mean salinity (a, b) and temperature (c, d) during the peak streamer period (July 6–7; a, c) and more typical shelfbreak frontal conditions (July 12–16; b, d) along the north-south transect at 70.8°W . Dashed and solid lines indicate the 34.5 psu isohaline (indicating the center of the frontal zone) and seafloor depth, respectively. All rates were measured within the euphotic zone ($>0.1\%$ surface PAR) at their respective stations.

respectively; Table S2 Supporting Information S1). Of these high rates, one occurred in surface waters in the shelf streamer at the most offshore transect station (July 6; Figures 3a and 3c) and another in surface waters at the edge of the warm core ring adjacent to the streamer (salinity = 34.2 psu; July 8; Figure S5 in Supporting Information S1). The other two exceptionally high rates were measured in shelf waters near the shelfbreak front after the streamer had migrated away from the north-south transect (July 16; Figures 3b and 3d)—one at the surface and the other at the top of the chlorophyll *a* maximum (21 m below surface), which overrode a finger of moderate salinity (~34.1 psu) water.

Elevated N_2 fixation rates ($10\text{--}100 \text{ nmol N L}^{-1} \text{d}^{-1}$) were observed throughout the study region in the warm, stratified surface waters ($>18^\circ\text{C}$, $<5 \text{ m}$) across all water masses and the frontal zone (Figure 3a, Figure S6 in Supporting Information S1). In these stratified surface waters, 97.0% of replicated samples were above the detection limit, and 90.9% were considered quantifiable; the median N_2 fixation rate was $27.2 \text{ nmol N L}^{-1} \text{d}^{-1}$ ($n = 33$). This pattern in N_2 fixation rates was driven by an increase in the relative contribution of diazotrophs to PN turnover (i.e., in the specific N_2 uptake rate): In surface waters, specific N_2 uptake rates were elevated (Figure 2c; stratified surface waters exhibited $\sigma_T < 23$) while PN concentrations generally peaked deeper in the water column (Figure S7 in Supporting Information S1).

Though rare, elevated rates of N_2 fixation were observed below the surface mixed layer at two stations (39.880°N and 39.815°N , 70.830°W) along the cross-shelf (along-streamer) transect (July 6), occurring both immediately above ($\sim 25 \text{ m}$) and within ($\sim 40 \text{ m}$) the chlorophyll *a* maxima (Figures 3a and 3c). These samples were collected within streamer waters over the continental slope ($>200 \text{ m}$ seafloor depth), with the chlorophyll *a* maxima at both stations occurring within the frontal waters (34–35 psu) at the base of the streamer.

In samples collected throughout the euphotic zone, N_2 fixation rates were significantly higher in shelf ($p = 0.003$) and frontal waters ($p = 0.006$) when compared to offshore waters, with the highest median rate ($8.42 \text{ nmol N L}^{-1} \text{d}^{-1}$, $n = 13$) observed in frontal waters (Figure 2b; Table S2 in Supporting Information S1). The high N_2 fixation rates observed in shelf waters persisted during the streamer event as shelf waters were advected offshore (Figure 3), representing a substantive contribution of new N to the Slope Sea (see Section 3.3). Again, this trend was clearly driven by an increase in the relative contribution of diazotrophs to the PN pool. Specific uptake rates were significantly greater in shelf ($p = 0.047$) and frontal ($p = 0.007$) waters compared to the offshore water (Figure S8; Table S2 in Supporting Information S1) while PN concentrations were greater in the shelf water compared to both the frontal ($p < 0.001$) and offshore ($p = 0.005$; Figure 2d; Table S2 in Supporting Information S1) waters.

3.3. Offshore Flux of Fixed N Induced by the Streamer

PN concentrations on the shelf significantly exceed those on the slope (Table S2 in Supporting Information S1); consequently, the streamer event resulted in a net influx of PN to the Slope Sea. In streamer waters (i.e., waters with salinity <34.5 present at stations offshore of the shelfbreak i.e., the 200 m isobath) sampled on July 6–7, the median concentration of PN was $1.47 \mu\text{M}$ ($n = 61$). In comparable offshore waters (<50 m sample depth), the median PN concentration was $0.68 \mu\text{M}$ ($n = 169$). By integrating shipboard velocity (ADCP) data across the cross-sectional area of the streamer (as defined by the 34.5 isohaline), Zhang et al. (2023) estimate that the offshore volume flux of shelf water induced by the streamer was $0.26 \times 10^6 \text{ m}^3 \text{ s}^{-1}$ at the time of our cross-streamer transect (July 8). Assuming an equal exchange of mass volume between the shelf and offshore waters (to conserve the shelf volume; a conservative approach to estimating the net flux), we calculate an instantaneous net offshore PN flux of 248 mton d^{-1} (or $2.48 \times 10^{-4} \text{ Tg N d}^{-1}$). If, conversely, the shelf volume were conserved completely by a southward inflow of upstream shelf waters from the north (i.e., no onshore transport of the offshore water), the net PN flux could have been as high as 462 mton d^{-1} . These values offer upper and lower bounds and likely bracket the true PN flux.

The streamer resulted in an influx of newly fixed N to the slope as shelf-water diazotrophs were advected offshore. Based on satellite images of sea surface temperature and chlorophyll *a*, the streamer was roughly 200 km in length with a measured mean surface speed of $\sim 0.3 \text{ m s}^{-1}$ (Zhang et al., 2023). From this, we calculate a residence time (i.e., before mixing with offshore waters) of shelf water in the streamer of roughly 8 days. Given an offshore volume flux of $0.26 \times 10^6 \text{ m}^3 \text{ s}^{-1}$ (Zhang et al., 2023), the instantaneous offshore volume of the streamer was approximately $2 \times 10^{11} \text{ m}^3$. In the 2 days (July 6–7) of our repeated streamer sampling, the median N_2 fixation rate in the streamer water was $20.7 \text{ nmol N L}^{-1} \text{ d}^{-1}$ ($n = 17$). (We note that this was not significantly different from N_2 fixation rates in the shelf water ($n = 63$) measured throughout the cruise (one-way ANOVA, $F = 0.225$, $p = 0.645$)). Assuming that diazotrophs in shelf waters cease activity once fully mixed into offshore waters, we calculate an input of 58 mton of newly fixed N d^{-1} (or $5.8 \times 10^{-5} \text{ Tg N d}^{-1}$) into the Slope Sea through the streamer. If the shelf volume was conserved by the onshore intrusion of offshore seawater with less active diazotrophs communities (median N_2 fixation rate = $2.59 \text{ nmol N L}^{-1} \text{ d}^{-1}$, $n = 33$), we calculate that the two-way exchange processes result in a net flux of 51 mton N d^{-1} to the Slope Sea. These values are equivalent to 20.5% and 12.5% of the upper and lower PN flux estimates, respectively. Moreover, these values represent 6.6% and 7.6%, respectively, of the mean daily N_2 fixed across the entire MAB and Gulf of Maine shelf area (Mulholland et al., 2019).

3.4. Diazotrophic Communities

N_2 fixation rates measured across the transect were associated with a mixed diazotroph community based on *nifH* quantification of common diazotrophic clades (Figure 4; Table S3). Under the more typical shelfbreak frontal conditions that followed the streamer event (July 14–15), only UCYN-A1 and UCYN-A2—two sublineages of the unicellular cyanobacterium *Atellocyanobacterium thalassa*—were observed in shelf waters (Figure 4a). These diazotrophs were also observed in frontal, offshore, and ring waters where *Trichodesmium* spp. and *R. euintracellularis* (i.e., Het-2; a heterocystous cyanobacterial symbiont of the diatom *Hemiaulus*) also abounded (Figures 4b–4d and 4f). Abundances of the UCYN-A groups were generally highest in surface waters and declined with depth. In contrast, Het-2 and *Trichodesmium* remained elevated above and within the chlorophyll *a* maxima at the shelfbreak front (Figure 4b) and in offshore waters (Figure 4c).

During the streamer event, we observed a general increase in the abundance of UCYN-A1, UCYN-A2, and *Trichodesmium* in surface waters with distance from the separation point, with Het-2 appearing offshore (Figures 4g and 4e). Commensurate with this increase in abundance, surface phosphate concentrations decreased from 0.1 to $\sim 0.05 \mu\text{M}$ offshore, while nitrate remained undetectable throughout (Table S3). To the east and west of the streamer, we observed the added presence of *R. rhizosoleniae* (Het-3; a symbiont of the diatom *Chaetoceros*) in surface waters. Interestingly, none of these diazotrophs were detected at the most inshore station in the streamer (40.464°N , 70.830°W) despite high rates of N_2 fixation observed in surface waters there (Figures 2a and 2c). This apparent discrepancy could be due to the presence of diazotrophic clades whose abundances were not assessed in this study. Non-cyanobacterial diazotrophs, for example, have been previously observed on the inner continental shelf (Mulholland et al., 2019) and UCYN-B has been observed at low abundance in the western North Atlantic (Ratten et al., 2015).

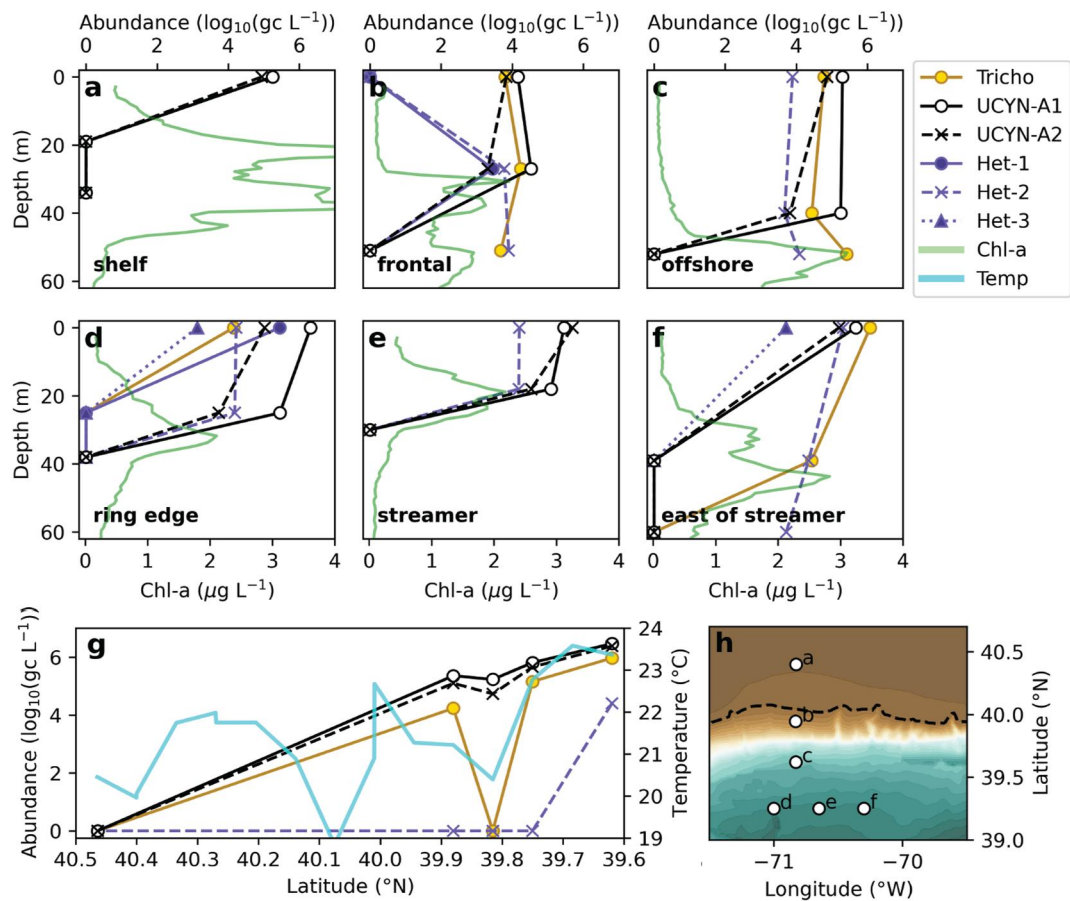


Figure 4. Abundances (copies L^{-1} of *nifH* genes) of several common diazotrophic clades across the shelfbreak front during relaxed ((a–c); July 14–15) and streamer ((d–g); July 6–8) conditions. The following diazotrophs were surveyed: *Trichodesmium* spp. (yellow), the haptophyte symbionts UCYN-A1 and UCYN-A2 (black), and the diatom symbionts *Richelia intracellularis* (Het-1, a symbiont of *Rhizosolenia* spp.), *Richelia euintracellularis* (Het-2, a symbiont of *Hemiaulus* spp.), and *Richelia rhizosoleniae* (Het-3, a symbiont of *Chaetoceros* spp.; purple). Station locations (h) are shown overlying seafloor depth; dashed line indicates the 200 m isobath.

4. Discussion

4.1. Elevated N_2 Fixation Rates in Shelf Waters

Much recent discussion has been centered on whether significant inputs of new N via N_2 fixation occur on continental shelves where terrestrial inputs of fixed N were once presumed to preclude significant diazotrophy. The work presented here, in addition to other recent research (Mulholland et al., 2012, 2019; Selden, Chappell, et al., 2021; Tang et al., 2019, 2020), has demonstrated that the answer is unequivocally “yes” for at least part of the western North Atlantic continental shelf. Here, we show that not only was the absolute flux of newly fixed N greater in shelf waters, but the relative contribution of diazotrophs to community N turnover was higher as well (Table S2 and Figure S8 in Supporting Information S1), suggesting that diazotrophic contributions are important in supporting productivity on the shelf. Assessing diazotrophic contributions and their physicochemical drivers in this system has bearing not only on the regional N budget, but on our understanding of N_2 fixation in continental shelf systems globally, particularly those impacted by western boundary currents (e.g., Jiang et al., 2023; Marshall et al., 2023) where diazotrophy has been observed for decades (e.g., Prufert-Bebout et al., 1993; Saino & Hattori, 1978). Our findings call for greater focus on shelf environments as regions of N_2 fixation and contributors to the global N budget, and for a paradigm shift regarding the relative importance of N_2 fixation in fueling productivity near the coast.

4.2. Weak Sensitivity of Coastal Communities to Fixed N

In nearly a third of samples ($n = 21$) where N_2 fixation was detectable ($n = 77$), nitrate concentrations were $>1 \mu\text{M}$ (Figures S9 and S10 in Supporting Information S1; Table S1). In these samples, N_2 fixation rates were elevated ($>10 \text{ nmol N L}^{-1} \text{ d}^{-1}$) only where phosphate was also elevated ($>0.4 \mu\text{M}$; Figure S9 in Supporting Information S1; Table S1). Nitrate has historically been thought to preclude N_2 fixation; however, it has long been known that *Trichodesmium* can fix N_2 in the presence of dissolved inorganic N including nitrate (e.g., Mulholland & Capone, 2001; Mulholland et al., 2001; Ohki et al., 1991) and numerous subsequent reports of N_2 fixation in waters bearing nitrate (e.g., Grosse et al., 2010; Mulholland et al., 2012, 2019; Shiozaki et al., 2015; Sohm et al., 2011) has led to a revision of this paradigm (see Knapp, 2012). Indeed, UCYN-A appears to constitutively fix N_2 for its host and has even been observed to increase cell-specific N_2 fixation rates following nitrate amendments (Mills et al., 2020), while *R. intracellularis* (Het-1) and *R. euintracellularis* (Het-2) lack genes necessary to assimilate ammonium and nitrate (Caputo et al., 2019). Given the mixed diazotrophic community observed throughout our study region (Figure 4) and prior observations on the MAB shelf (Mulholland et al., 2012, 2019) demonstrating that nitrate concentrations characteristic of the region do not inhibit N_2 fixation, the relative insensitivity of N_2 fixation to nitrate should not be surprising. Nevertheless, the majority of water column N_2 fixation in this study occurred in the surface mixed layer where nitrate was drawn down throughout the study region. From this, we infer a weak relationship between fixed N availability and N_2 fixation (whereby fixed N does not preclude active diazotrophy provided sufficient phosphorus is available, but its absence favors diazotrophs within the population) in surface waters on the MAB shelf.

4.3. Frontal Conditions Favor Diazotrophy

Our results suggest that diazotrophs contribute a greater fraction of the N to support productivity under frontal conditions, including those observed at the shelfbreak front. Unlike in MAB shelf waters, frontal waters did not have significantly higher PN concentrations than offshore waters; yet, N_2 fixation rates there were significantly greater (Figure 2b; Table S2 in Supporting Information S1). Indeed, the median specific uptake rate in frontal waters ($1.15 \times 10^{-2} \text{ d}^{-1}$) was an order of magnitude higher than that observed in either shelf ($2.38 \times 10^{-3} \text{ d}^{-1}$) or offshore ($1.40 \times 10^{-3} \text{ d}^{-1}$) waters (Figure S8 and Table S2 in Supporting Information S1). This finding is highly suggestive of an enhancement in the relative contribution of N_2 fixation to the PN pool although we failed to find a statistically significant difference between specific N_2 uptake rates measured in shelf and frontal waters (Figure 2; Table S2 in Supporting Information S1), likely due to our small sampling size and the high variability observed in both water masses.

Enhanced diazotrophic contributions in frontal waters have previously been observed along the western North Atlantic continental shelf and in other western boundary current systems. For example, at the confluence of southward-flowing MAB shelf waters and northward-flowing Gulf Stream waters, Selden, Chappell, et al. (2021) observed exceptionally high N_2 fixation rates associated with the transport of UCYN-A offshore. Similarly, Lu et al. (2019) observed elevated N_2 fixation rates where South China sea waters mixed with a Kuroshio intrusion. The authors attribute this enhancement to the relief of nutrient limitation experienced by *Trichodesmium* in the oligotrophic Kuroshio intrusion as it mixes with coastal waters.

While we can only speculate as to why the relative importance of diazotrophs to community N demand was maximized at the shelfbreak in this study, one potential explanation is that denitrification draws down terrestrially sourced inorganic N concentrations across the shelf (Fennel et al., 2006), causing the ecological niche for N_2 fixation to expand with distance from the coast until iron, phosphorus, or another factor limits N_2 fixation. This idea is supported by the observation that both primary productivity, chlorophyll *a* concentrations, and nitracline depth tend to decrease across the shelf (Zhang et al., 2023). A second (and potentially additive) explanation is that upwelling stimulates N_2 fixation at the shelfbreak. Frontal dynamics are thought to drive upwelling of nutrient-rich slope waters with commensurate increases in productivity associated with fast-growing phytoplankton (e.g., diatoms; Allen et al., 2005; Mangolte et al., 2022; Zhang et al., 2013). We posit that certain endosymbiotic diazotrophs and their hosts may be well-poised to respond rapidly to nutrient injections, as observed for coastal UCYN-A strains in the other upwelling systems (e.g., Mills et al., 2020; Selden et al., 2022). Moreover, if upwelling is driven by water mass convergence in the bottom boundary layer, as has been previously hypothesized (Barth et al., 2004; Houghton & Vizbeck, 1998; Linder et al., 2004), then upwelled waters may carry iron (derived

from shelf sediments) into the euphotic zone, potentially relieving iron-limitation of N_2 fixation (Moore et al., 2009). Additional high-resolution sampling is necessary to untangle these potential mechanisms.

4.4. Streamer-Driven Transport of New N to the Slope Sea

We estimate that diazotrophs in the offshore-flowing shelf-water streamer injected 51–58 mtons of newly fixed N d^{-1} to the Slope Sea—equivalent to 12%–20% of the PN flux associated with the streamer at the time we observed it (Section 3.3). This finding supports the hypothesis that active diazotrophs transferred offshore by the streamer resulted in a considerable addition of new N to the Slope Sea. However, extrapolating beyond this particular streamer event is problematic because, while we can estimate streamer frequency based on remotely sensed data of surface salinity and temperature, there is high interannual and seasonal variability in the activity of diazotrophic communities in these coastal waters (Mulholland et al., 2019). Moreover, our instantaneous estimates of streamer volume and flux were based on in situ measurements; these values likely varied even over this streamer's lifetime.

The PN and newly fixed N fluxes that we report in association with the streamer were significant relative to regional estimates of cross-shelf N fluxes. For example, Friedrichs et al. (2018) estimated a mean cross-shelf flux of 1,370 mton d^{-1} ($\sim 0.5 \text{ Tg total N y}^{-1}$) from the MAB to the Slope Sea in a normal July. The PN flux from this single streamer event observed here was 248–462 mton d^{-1} , representing a significant fraction (18%–34%) of the total offshore N flux for the entire MAB region. Concurrent diazotrophic inputs added a further $\sim 4\%$ of N inputs currently unaccounted for in MAB regional N budgets (Fennel et al., 2006; Friedrichs et al., 2018). Because cross-shelf exchanges across the MAB shelf edge are likely to increase due to recent increases in the meandering of the Gulf Stream (Andres, 2016) and number of warm core rings being formed in the Slope Sea (Gangopadhyay et al., 2020), such episodic cross-shelf fluxes of newly fixed N may become increasingly frequent and important for the often N-limited North Atlantic basin (Moore et al., 2013).

5. Conclusions

Constraining the factors which regulate new N inputs via N_2 fixation remains both a challenge and a priority in oceanography—a challenge due to the diverse ecological roles and metabolic strategies employed by diazotrophs and a priority due to the potential for changing N budgets to affect carbon sequestration in the ocean. The results presented here contribute to a growing body of research which support two important paradigm shifts in the marine N cycle: (a) Diazotrophs on continental shelves contribute significantly to regional and global N budgets (e.g., Mulholland et al., 2019; Sipler et al., 2017); and (b) most diazotrophic consortia are not as sensitive to fixed N as previously thought (Knapp, 2012). But, most importantly, the work presented here demonstrates that frontal exchange significantly alters the flux and fate of newly fixed N. Indeed, diazotrophs entrained in the shelf-water streamer documented added $>50 \text{ mton N d}^{-1}$ to the Slope Sea—a value representing $\sim 4\%$ of the total N flux from the entire MAB continental shelf to the neighboring Slope Sea (Friedrichs et al., 2018) and $\sim 7\%$ of the mean amount of N_2 fixed daily across the entire MAB and Gulf of Maine shelf area (Mulholland et al., 2019). As N_2 fixation rates in other western boundary current systems like the Kuroshio are not only elevated (Wen et al., 2022), but also appear to be favored by frontal mixing (Lu et al., 2019), our findings suggest that (sub) mesoscale physical features at the ocean's margins may play an important role in controlling fixed N inputs via N_2 fixation to both shelf and offshore communities. As cross-shelf transport events induced by warm-core rings are likely to have increased due to recent western boundary current destabilization (Andres, 2016), the contribution of continental shelf diazotrophs and N export to regional N budgets in the MAB Slope Sea and comparable systems may rise, with consequences for marine productivity both locally and globally.

Data Availability Statement

CTD and sensor data are archived at the Biological and Chemical Oceanography Data Management Office (BCO-DMO) on the SPIROPA ('Shelfbreak Productivity Interdisciplinary Research Operation at the Pioneer Array') Project page: <https://www.bco-dmo.org/project/748894>. The MODIS Aqua sea surface temperature and chlorophyll *a* concentration data are publicly available courtesy of the NASA Goddard Space Flight Center: <https://oceancolor.gsfc.nasa.gov/>. All measurements required to calculate N_2 fixation rates, as well as calculated specific N_2 uptake and N_2 fixation rates, are available in the Supplemental Materials associated with this publication, and have been submitted for archival purposes to the BCO-DMO data repository.

Acknowledgments

We gratefully acknowledge NSF grant OCE-1657803 awarded to co-authors DM and WZ in collaboration with Heidi Sosik (WHOI), Jefferson Turner (UMass Dartmouth) and Christian Petipas (MA Division of Marine Fisheries) for supporting our oceanographic expedition and the collection of all hydrographic data presented here. We also acknowledge funding from the Old Dominion University Department of Ocean and Earth Sciences awarded to MRM, SC, and PDC for supporting the collection and analysis of samples and data pertaining to N₂ fixation rates as well as the Jeffress Trust Awards Program in Interdisciplinary Research for funding awarded to PDC which supported our assessment of diazotroph community composition. A big thanks to the captain and crew of the R/V *Thomas G. Thompson* for their support in sample collection, and to the SPIROPA team for their aid in the field and their thoughts on this manuscript. Thank you to Kim Powell (ODU) for her assistance in *nifH* analysis, to Christopher Powell (ODU) for his input in designing our on-deck chiller system, and to Olga Kosnyrev (WHOI) for curating the hydrographic data produced during the SPIROPA project. Thank you as well to Walker Smith and Meredith Meyers (VIMS) for providing additional particulate organic N concentration data. Finally, CRS thanks Nathan Yee (Rutgers University) for supporting her time during the preparation of this manuscript. Thanks also to Associate Editors Dr. Löscher and Dr. Foster and to the anonymous reviewers whose comments helped us improve the manuscript.

References

Allen, J., Brown, L., Sanders, R., Moore, C. M., Mustard, A., Fielding, S., et al. (2005). Diatom carbon export enhanced by silicate upwelling in the northeast Atlantic. *Nature*, 437(7059), 728–732. <https://doi.org/10.1038/nature03948>

Andres, M. (2016). On the recent destabilization of the Gulf Stream path downstream of Cape Hatteras. *Geophysical Research Letters*, 43(18), 9836–9842. <https://doi.org/10.1002/2016GL069966>

Barth, J., Herbert, D., Dale, A., & Ullman, D. (2004). Direct observations of along-isopycnal upwelling and diapycnal velocity at a shelfbreak front. *Journal of Physical Oceanography*, 34(3), 543–565. <https://doi.org/10.1175/2514.1>

Bourbonnais, A., Lehmann, M. F., Waniek, J. J., & Schulz-Bull, D. E. (2009). Nitrate isotope anomalies reflect N₂ fixation in the Azores Front region (subtropical NE Atlantic). *Journal of Geophysical Research*, 114(C3). <https://doi.org/10.1029/2007JC004617>

Bustin, S. A., Mueller, R., & Nolan, T. (2020). Parameters for successful PCR primer design. *Quantitative Real-Time PCR: Methods and Protocols*, 5–22.

Capone, D. G., Burns, J. A., Montoya, J. P., Subramaniam, A., Mahaffey, C., Gunderson, T., et al. (2005). Nitrogen fixation by Trichodesmium spp.: An important source of new nitrogen to the tropical and subtropical North Atlantic Ocean. *Global Biogeochemical Cycles*, 19(2). <https://doi.org/10.1029/2004GB002331>

Capone, D. G., Zehr, J. P., Paerl, H. W., Bergman, B., & Carpenter, E. J. (1997). Trichodesmium, a globally significant marine cyanobacterium. *Science*, 276(5316), 1221–1229. <https://doi.org/10.1126/science.276.5316.1221>

Caputo, A., Nylander, J. A., & Foster, R. A. (2019). The genetic diversity and evolution of diatom-diazotroph associations highlights traits favoring symbiont integration. *FEMS Microbiology Letters*, 366(2), fny297. <https://doi.org/10.1093/femsle/fny297>

Carpenter, E. J., Montoya, J. P., Burns, J., Mulholland, M. R., Subramaniam, A., & Capone, D. G. (1999). Extensive bloom of a N₂-fixing diatom/cyanobacterial association in the tropical Atlantic Ocean. *Marine Ecology Progress Series*, 185, 273–283. <https://doi.org/10.3354/meps185273>

Chang, B. X., Jayakumar, A., Widner, B., Bernhardt, P., Mordy, C. W., Mulholland, M. R., & Ward, B. B. (2019). Low rates of dinitrogen fixation in the eastern tropical South Pacific. *Limnology & Oceanography*, 64(5), 1913–1923. <https://doi.org/10.1002/lo.11159>

Church, M. J., Jenkins, B. D., Karl, D. M., & Zehr, J. P. (2005). Vertical distributions of nitrogen-fixing phylotypes at Stn ALOHA in the oligotrophic North Pacific Ocean. *Aquatic Microbial Ecology*, 38(1), 3–14. <https://doi.org/10.3354/ame038003>

Clayton, S., Nagai, T., & Follows, M. (2014). Fine scale phytoplankton community structure across the Kuroshio Front. *Journal of Plankton Research*, 36(4), 1017–1030. <https://doi.org/10.1093/plankt/fbu020>

Dugdale, R., Menzel, D. W., & Ryther, J. H. (1961). Nitrogen fixation in the Sargasso Sea. *Deep-Sea Research*, 7(4), 298–300. [https://doi.org/10.1016/0146-6313\(61\)90051-x](https://doi.org/10.1016/0146-6313(61)90051-x)

Dugdale, R. C., Goering, J. J., & Ryther, J. H. (1964). High nitrogen fixation rates in the Sargasso sea and the arabian sea 1. *Limnology & Oceanography*, 9(4), 507–510. <https://doi.org/10.4319/lo.1964.9.4.0507>

Falkowski, P. G., Barber, R. T., & Smetacek, V. (1998). Biogeochemical controls and feedbacks on ocean primary production. *Science*, 281(5374), 200–206. <https://doi.org/10.1126/science.281.5374.200>

Fennel, K., Wilkin, J., Levin, J., Moisan, J., O'Reilly, J., & Haidvogel, D. (2006). Nitrogen cycling in the Middle Atlantic Bight: Results from a three-dimensional model and implications for the North Atlantic nitrogen budget. *Global Biogeochemical Cycles*, 20(3). <https://doi.org/10.1029/2005GB002456>

Foster, R., Subramaniam, A., Mahaffey, C., Carpenter, E., Capone, D., & Zehr, J. (2007). Influence of the Amazon River plume on distributions of free-living and symbiotic cyanobacteria in the western tropical North Atlantic Ocean. *Limnology & Oceanography*, 52(2), 517–532. <https://doi.org/10.4319/lo.2007.52.2.0517>

Friedrichs, M. A., St-Laurent, P., Xiao, Y., Hofmann, E., Hyde, K., Mannino, A., et al. (2018). Ocean circulation causes strong variability in Mid-Atlantic Bight net community production. *JGR Oceans*, 124(1), 113–134. <https://doi.org/10.1029/2018JC014424>

Gangopadhyay, A., Gawarkiewicz, G., Nishchitha, E., Silva, S., Silver, A. M., Monim, M., & Clark, J. (2020). A census of the warm-core rings of the Gulf Stream: 1980–2017. *Journal of Geophysical Research: Oceans*, 125(8), e2019JC016033. <https://doi.org/10.1029/2019JC016033>

Gawarkiewicz, G., Ferdelman, T. G., Church, T. M., & Luther III, G. W. (1996). Shelfbreak frontal structure on the continental shelf north of Cape Hatteras. *Continental Shelf Research*, 16(14), 1751–1773. [https://doi.org/10.1016/0278-4343\(96\)00014-3](https://doi.org/10.1016/0278-4343(96)00014-3)

Gawarkiewicz, G., Todd, R. E., Zhang, W., Partida, J., Gangopadhyay, A., Monim, M.-U.-H., et al. (2018). The changing nature of shelf-break exchange revealed by the OOI Pioneer Array. *Oceanography*, 31(1), 60–70. <https://doi.org/10.5670/oceanog.2018.110>

Grosse, J., Bombar, D., Doan, H., Nguyen, L., & Voss, M. (2010). The Mekong River plume fuels nitrogen fixation and determines phytoplankton species distribution in the South China Sea during low and high discharge season. *Limnology and Oceanography*, 55(4), 1668–1680. <https://doi.org/10.4319/lo.2010.55.4.1668>

Gruber, N. (2004). The dynamics of the marine nitrogen cycle and its influence on atmospheric CO₂ variations. *The Ocean Carbon Cycle and Climate*, 97–148. Springer. https://doi.org/10.1007/978-1-4020-2087-2_4

Gruber, N., & Galloway, J. N. (2008). An Earth-system perspective of the global nitrogen cycle. *Nature*, 451(7176), 293–296. <https://doi.org/10.1038/nature06592>

Houghton, R., & Vizbeck, M. (1998). Upwelling and convergence in the middle Atlantic Bight shelfbreak front. *Geophysical Research Letters*, 25(15), 2765–2768. <https://doi.org/10.1029/98gl02105>

Hutchins, D., Fu, F.-X., Zhang, Y., Warner, M., Feng, Y., Portune, K., et al. (2007). CO₂ control of Trichodesmium N₂ fixation, photosynthesis, growth rates, and elemental ratios: Implications for past, present, and future ocean biogeochemistry. *Limnology & Oceanography*, 52(4), 1293–1304. <https://doi.org/10.4319/lo.2007.52.4.1293>

Jiang, Z., Zhu, T., Sun, Z., Zhai, H., Zhou, F., Yan, X., et al. (2023). Enhancement of summer nitrogen fixation by the Kuroshio intrusion in the East China Sea and Southern Yellow Sea. *JGR: Biogeosciences*, 128(3), e2022JG007287. <https://doi.org/10.1029/2022JG007287>

Joyce, T. M., Bishop, J. K., & Brown, O. B. (1992). Observations of offshore shelf-water transport induced by a warm-core ring. *Deep-Sea Research, Part A: Oceanographic Research Papers*, 39, S97–S113. [https://doi.org/10.1016/S0198-0149\(11\)80007-5](https://doi.org/10.1016/S0198-0149(11)80007-5)

Klawonn, I., Lavik, G., Böning, P., Marchant, H. K., Dekaezemacker, J., Mohr, W., & Ploug, H. (2015). Simple approach for the preparation of ¹⁵N₂-enriched water for nitrogen fixation assessments: Evaluation, application and recommendations. *Frontiers in Microbiology*, 6, 769. <https://doi.org/10.3389/fmicb.2015.00769>

Knapp, A. N. (2012). The sensitivity of marine N₂ fixation to dissolved inorganic nitrogen. *Frontiers in Microbiology*, 3, 374. <https://doi.org/10.3389/fmicb.2012.00374>

Linder, C. A., Gawarkiewicz, G., & Pickart, R. (2004). Seasonal characteristics of bottom boundary layer detachment at the shelfbreak front in the Middle Atlantic Bight. *Journal of Geophysical Research*, 109(C3). <https://doi.org/10.1029/2003JC002032>

Linder, C. A., & Gawarkiewicz, G. G. (1998). A climatology of the shelfbreak front in the Middle Atlantic Bight. *Journal of Geophysical Research*, 103(C9), 18405–18423. <https://doi.org/10.1029/98JC01438>

Lu, Y., Wen, Z., Shi, D., Lin, W., Bonnet, S., Dai, M., & Kao, S. (2019). Biogeography of N₂ fixation influenced by the western boundary current intrusion in the South China Sea. *Journal of Geophysical Research: Oceans*, 124(10), 6983–6996. <https://doi.org/10.1029/2018JC014781>

Mahaffey, C., Michaels, A. F., & Capone, D. G. (2005). The conundrum of marine N₂ fixation. *American Journal of Science*, 305(6–8), 546–595. <https://doi.org/10.2475/ajs.305.6-8.546>

Mangolte, I., Lévy, M., Dutkiewicz, S., Clayton, S., & Jahn, O. (2022). Plankton community response to fronts: Winners and losers. *Journal of Plankton Research*, 44(2), 241–258. <https://doi.org/10.1093/plankt/fbac010>

Manly, B. F. (2006). *Randomization, bootstrap and Monte Carlo methods in biology* (Vol. 70). CRC press.

Marshall, T., Sigman, D., Beal, L., Foreman, A., Martínez-García, A., Blain, S., et al. (2023). The Agulhas Current transports signals of local and remote Indian Ocean nitrogen cycle. *Journal of Geophysical Research: Oceans*, 128(3), e2022JC019413. <https://doi.org/10.1029/2022JC019413>

Mills, M. M., Turk-Kubo, K. A., van Dijken, G. L., Henke, B. A., Harding, K., Wilson, S. T., et al. (2020). Unusual marine cyanobacteria/haptophyte symbiosis relies on N₂ fixation even in N-rich environments. *The ISME Journal*, 14(10), 2395–2406. <https://www.doi.org/s41396-020-0691-6>

Montoya, J. P., Voss, M., Kahler, P., & Capone, D. G. (1996). A simple, high-precision, high-sensitivity tracer assay for N₂ fixation. *Applied and Environmental Microbiology*, 62(3), 986–993. <https://doi.org/10.1128/aem.62.3.986-993.1996>

Moore, C. M., Mills, M., Achterberg, E., Geider, R., LaRoche, J., Lucas, M., et al. (2009). Large-scale distribution of Atlantic nitrogen fixation controlled by iron availability. *Nature Geoscience*, 2(12), 867–871. <https://doi.org/10.1038/ngeo667>

Moore, C. M., Mills, M., Arrigo, K., Berman-Frank, I., Bopp, L., Boyd, P., et al. (2013). Processes and patterns of oceanic nutrient limitation. *Nature Geoscience*, 6(9), 701–710. <https://doi.org/10.1038/ngeo1765>

Mulholland, M. R., Bernhardt, P., Blanco-Garcia, J., Mannino, A., Hyde, K., Mondragon, E., et al. (2012). Rates of dinitrogen fixation and the abundance of diazotrophs in North American coastal waters between Cape Hatteras and Georges Bank. *Limnology & Oceanography*, 57(4), 1067–1083. <https://doi.org/10.4319/lo.2012.57.4.1067>

Mulholland, M. R., Bernhardt, P. W., Widner, B. N., Selden, C. R., Chappell, P. D., Clayton, S., et al. (2019). High rates of N₂ fixation in temperate, western North Atlantic coastal waters expand the realm of marine diazotrophy. *Global Biogeochemical Cycles*, 33(7), 826–840. <https://doi.org/10.1029/2018GB006130>

Mulholland, M. R., & Capone, D. G. (2000). The nitrogen physiology of the marine N₂-fixing cyanobacteria *Trichodesmium* spp. *Trends in Plant Science*, 5(4), 148–153. [https://doi.org/10.1016/S1360-1385\(00\)01576-4](https://doi.org/10.1016/S1360-1385(00)01576-4)

Mulholland, M. R., & Capone, D. G. (2001). Stoichiometry of nitrogen and carbon utilization in cultured populations of *Trichodesmium* IMS101: Implications for growth. *Limnology & Oceanography*, 46(2), 436–443. <https://doi.org/10.4319/lo.2001.46.2.0436>

Mulholland, M. R., Ohki, K., & Capone, D. G. (2001). Nutrient controls on nitrogen uptake and metabolism by natural populations and cultures of *Trichodesmium* (Cyanobacteria). *Journal of Phycology*, 37(6), 1001–1009. <https://doi.org/10.1046/j.1529-8817.2001.00080.x>

NASA Goddard Space Flight Center, Ocean ecology laboratory, Ocean biology processing group. (2018). *Sea-viewing Wide Field-of-view Sensor (SeaWiFS) Ocean Color Data*. March 27, 2023 Retrieved from <https://oceancolor.gsfc.nasa.gov/>

Nixon, S., Ammerman, J., Atkinson, L., Berounsky, V., Billen, G., Boicourt, W., et al. (1996). The fate of nitrogen and phosphorus at the land-sea margin of the North Atlantic Ocean. *Biogeochemistry*, 35(1), 141–180. <https://doi.org/10.1007/bf02179826>

Ohki, K., Zehr, J. P., Falkowski, P. G., & Fujita, Y. (1991). Regulation of nitrogen-fixation in the marine nonheterocystous Cyanobacterium *Trichodesmium* sp Nibb1067. *Archives of Microbiology*, 156(5), 335–337. <https://doi.org/10.1007/bf00248706>

Oliver, H., Zhang, W. G., Smith Jr, W. O., Alatalo, P., Chappell, P. D., Hirzel, A. J., et al. (2021). Diatom hotspots driven by western boundary current instability. *Geophysical Research Letters*, 48(11), e2020GL091943. <https://doi.org/10.1029/2020GL091943>

Palter, J. B., Marinov, I., Sarmiento, J. L., & Gruber, N. (2013). Large-scale, persistent nutrient fronts of the World Ocean: Impacts on biogeochemistry. In *The handbook of environmental chemistry*. Springer. https://doi.org/10.1007/698_2013_241

Prufert-Bebout, L., Paerl, H., & Lassen, C. (1993). Growth, nitrogen fixation, and spectral attenuation in cultivated *Trichodesmium* species. *Environmental Microbiology*, 5(5), 1367–1375. <https://doi.org/10.1128/aem.59.5.1367-1375.1993>

Ratten, J., LaRoche, J., Desai, D., Shelley, R., Landing, W., Boyle, E., et al. (2015). Sources of iron and phosphate affect the distribution of diazotrophs in the North Atlantic. *Deep Sea Research Part II: Topical Studies in Oceanography*, 116, 332–341. <https://doi.org/10.1016/j.dsr2.2014.11.012>

Ripp, J. (1996). Analytical detection limit guidance and laboratory guide for determining method detection limits. *Wisconsin Department of Natural Resources, Laboratory Certification Program*.

Saino, T., & Hattori, A. (1978). Diel variation in nitrogen fixation by a marine blue-green alga, *Trichodesmium thiebautii*. *Deep-Sea Research*, 25(12), 1259–1263. [https://doi.org/10.1016/0146-6291\(78\)90019-x](https://doi.org/10.1016/0146-6291(78)90019-x)

Schvarcz, C. R., Wilson, S. T., Caffin, M., Stancheva, R., Li, Q., Turk-Kubo, K. A., et al. (2022). Overlooked and widespread pennate diatom-diazotroph symbioses in the sea. *Nature Communications*, 13(1), 799. <https://www.doi.org/s41467-022-28065-6>

Selden, C., Mulholland, M., Bernhardt, P., Widner, B., Macías-Tapia, A., Ji, Q., & Jayakumar, A. (2019). Dinitrogen fixation across physico-chemical gradients of the Eastern Tropical North Pacific oxygen deficient zone. *Global Biogeochemical Cycles*, 33(9), 1187–1202. <https://doi.org/10.1029/2019GB006242>

Selden, C. R., Chappell, P. D., Clayton, S., Macías-Tapia, A., Bernhardt, P. W., & Mulholland, M. R. (2021). A coastal N₂ fixation hotspot at the Cape Hatteras front: Elucidating spatial heterogeneity in diazotroph activity via supervised machine learning. *Limnology & Oceanography*, 66(5), 1832–1849. <https://doi.org/10.1002/lnco.11727>

Selden, C. R., Einarsson, S. V., Lowry, K. E., Crider, K. E., Pickart, R. S., Lin, P., et al. (2022). Coastal upwelling enhances abundance of a symbiotic diazotroph (UCYN-A) and its haptophyte host in the Arctic Ocean. *Frontiers in Marine Science*, 9. <https://doi.org/10.3389/fmars.2022.877562>

Selden, C. R., Mulholland, M. R., Widner, B., Bernhardt, P., & Jayakumar, A. (2021). Toward resolving disparate accounts of the extent and magnitude of nitrogen fixation in the Eastern Tropical South Pacific oxygen deficient zone. *Limnology & Oceanography*, 66(5), 1950–1960. <https://doi.org/10.1002/lnco.11735>

Shiozaki, T., Nagata, T., Ijichi, M., & Furuya, K. (2015). Nitrogen fixation and the diazotroph community in the temperature coastal region of the northwestern North Pacific. *Biogeosciences*, 12(15), 4751–4764. <https://doi.org/10.5194/bg-12-4751-2015>

Sipler, R. E., Gong, D., Baer, S. E., Sanderson, M. P., Roberts, Q. N., Mulholland, M. R., & Bronk, D. A. (2017). Preliminary estimates of the contribution of Arctic nitrogen fixation to the global nitrogen budget. *Limnology and Oceanography Letters*, 2(5), 159–166. <https://doi.org/10.1002/ol.201046>

Sohn, J., Hilton, J., Noble, A., Zehr, J., Saito, M., & Webb, E. (2011). Nitrogen fixation in the South Atlantic Gyre and the Benguela upwelling system. *Geophysical Research Letters*, 38(16). <https://doi.org/10.1029/2011GL048315>

Tang, W., Cerdán-García, E., Berthelot, H., Polyviou, D., Wang, S., Baylay, A., et al. (2020). New insights into the distributions of nitrogen fixation and diazotrophs revealed by high-resolution sensing and sampling methods. *The ISME Journal*, 14(10), 2514–2526. <https://www.doi.org/s41396-020-0703-6>

Tang, W., Wang, S., Fonseca-Batista, D., Dehairs, F., Gifford, S., Gonzalez, A. G., et al. (2019). Revisiting the distribution of oceanic N_2 fixation and estimating diazotrophic contribution to marine production. *Nature Communications*, 10(1), 831. <https://www.doi.org/s41467-019-08640-0>

Thompson, A., Carter, B. J., Turk-Kubo, K., Malfatti, F., Azam, F., & Zehr, J. P. (2014). Genetic diversity of the unicellular nitrogen-fixing cyanobacteria UCYN-A and its prymnesiophyte host. *Environmental Microbiology*, 16(10), 3238–3249. <https://doi.org/10.1111/1462-2920.12490>

Thompson, A. W., Foster, R. A., Krupke, A., Carter, B. J., Musat, N., Vaulot, D., et al. (2012). Unicellular cyanobacterium symbiotic with a single-celled eukaryotic alga. *Science*, 337(6101), 1546–1550. <https://doi.org/10.1126/science.1222700>

Voss, M., Bombar, D., Loick, N., & Dippner, J. W. (2006). Riverine influence on nitrogen fixation in the upwelling region off Vietnam, South China Sea. *Geophysical Research Letters*, 33(7). <https://doi.org/10.1029/2005GL025569>

Wen, Z., Browning, T. J., Cai, Y., Dai, R., Zhang, R., Du, C., et al. (2022). Nutrient regulation of biological nitrogen fixation across the tropical western North Pacific. *Science Advances*, 8(5), eab17564. <https://doi.org/10.1126/sciadv.abf17564>

White, A. E., Granger, J., Selden, C., Gradoville, M. R., Potts, L., Bourbonnais, A., et al. (2020). A critical review of the $^{15}N_2$ tracer method to measure diazotrophic production in pelagic ecosystems. *Limnology and Oceanography: Methods*, 18(4), 129–147. <https://doi.org/10.1002/lom3.10353>

Zehr, J. P., & Capone, D. G. (2020). Changing perspectives in marine nitrogen fixation. *Science*, 368(6492), eaay9514. <https://doi.org/10.1126/science.aay9514>

Zhang, W., Alatalo, P., Crockford, T., Hirzel, A. J., Meyer, M. G., Oliver, H., et al. (2023). Cross-shelf exchange associated with a shelf-water streamer at the Mid-Atlantic Bight shelf edge. *Progress in Oceanography*, 210, 102931. <https://doi.org/10.1016/j.pocean.2022.102931>

Zhang, W., & Gawarkiewicz, G. G. (2015a). Dynamics of the direct intrusion of Gulf Stream ring water onto the Mid-Atlantic Bight shelf. *Geophysical Research Letters*, 42(18), 7687–7695. <https://doi.org/10.1002/2015GL065530>

Zhang, W., & Gawarkiewicz, G. G. (2015b). Length scale of the finite-amplitude meanders of shelfbreak fronts. *Journal of Physical Oceanography*, 45(10), 2598–2620. <https://doi.org/10.1175/JPO-D-14-0249.1>

Zhang, W., McGillicuddy, D., & Gawarkiewicz, G. (2013). Is biological productivity enhanced at the New England shelfbreak front? *Journal of Geophysical Research Plus: Oceans*, 118(1), 517–535. <https://doi.org/10.1002/jgrc.20068>